

**HEPCAT Annual Report**  
**Rene M Padilla**  
**March 31, 2024**

In this annual progress report, I am presenting my ongoing work in the areas of Accelerator Diagnostic Physics and R&D in instrumentation. My work concentrates primarily on the implementation of single-crystalline diamond-based detector diagnostics for high-intensity, high-repetition rate X-ray Free Electron Lasers (XFELs) sources. This work has crucial impact to the solid-state sensor community and will help surpass the state-of-the-art efforts to create the next generation of accelerator diagnostic physics. My contributions include studies of radiation hardness tolerance, position sensitivity resolution using multi-pixel sensors, charge collection efficiency and signal propagation speed, and 3D high frequency simulations to understand how we can develop a multi-GHz diagnostic system.

**Radiation Tolerance of Solid-State Sensor**

I participated in an experiment aiming to explore the radiation hardness of single crystalline diamond devices. For this task, we exposed a diamond sensor to the proton beam at the Crocker Nuclear Laboratory (CNL) cyclotron located at UC Davis. The goal was to measure real time radiation damage of the diamond sensor fabricated by the Center for Integrated Nanotechnologies (CINT). The sensor was irradiated to a total dose of  $4 \times 10^{16}$  protons/cm<sup>2</sup>. This represents approximately four times the lifetime dose expected to be delivered by the Submersible Wireless Imaging Monitor (SWIM) diagnostic, which is the project this sensor was manufactured for. From this study, we obtained a real-time measurement of the degradation of diamond when exposed to ionized charges. However, to complete the study, we needed to measure the performance of the diamond sensor without having been exposed to any dose. This would give us the standard scale efficiency of these diamond sensors. For this, I went to SLAC National Laboratory and by making use of the X-ray Pump Probe (XPP) beamline, I exposed two back-to-back diamond devices to an energetic X-ray beam. One device held the irradiated diamond sensor while the second one had a non-irradiated sensor. Figure 1 shows the results from this study in which we observed that the diamonds sensor charge collection efficiency remains at about 24% for a total dose of  $4 \times 10^{16}$  protons/cm<sup>2</sup> and about 60% for a dose of  $1 \times 10^{16}$  protons/cm<sup>2</sup>. This demonstrated that diamond has a high radiation tolerance, and it can perform well for doses not exceeding  $1 \times 10^{15}$  protons/cm<sup>2</sup>.

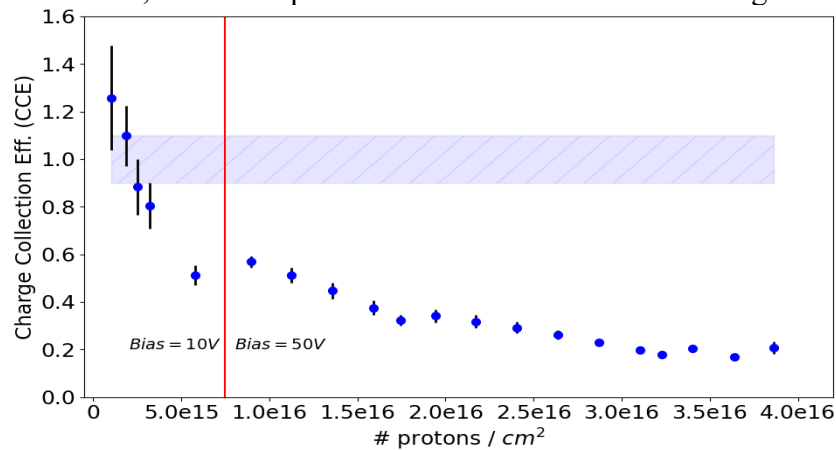


Figure 1: Single crystalline diamond sensor irradiated performance. Charge collection efficiency as a function of irradiated proton fluence.

## Position Sensitivity of Solid-State Sensors

Another aspect of my research is to use diamond sensors to measure the position sensitivity of a XFEL. This task can be approached by sliding a single channel diamond sensor into a multi-pixel device. Figure 2 shows a diagram of a four-channel diamond sensor where each gray square represents an electrode conductor. With this configuration, a readout system can be connected to each one of the electrodes allowing us to measure the charge generated inside of the diamond bulk.

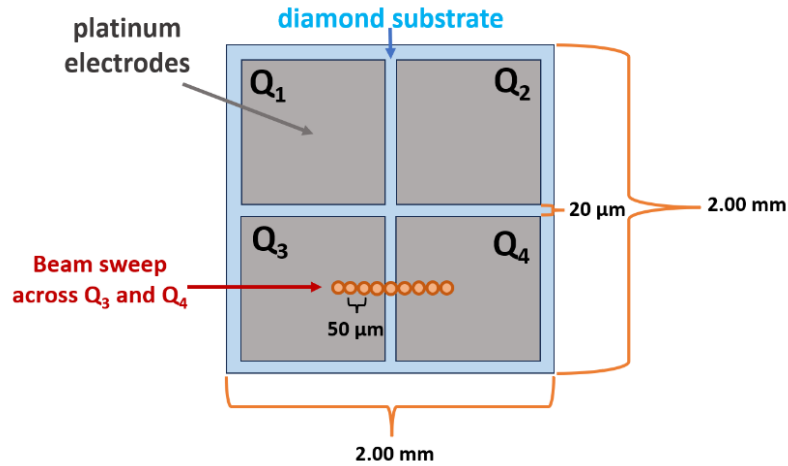


Figure 2: Diagram of the four-quadrant diamond sensor used to measure the position resolution of the XPP X-ray beam at SLAC.

Since diamond-based sensors enable us to collect charges at a rate of 200  $\mu\text{m}/\text{ns}$  when they reach saturation, I designed a readout system that would allow us to stretch the output pulses for about 20 ns. The reason for this is to have a system capable of performing X-ray position measurements at a repetition rate of about 20 MHz. However, the prototype described here can read X-ray pulses at the 50 MHz repetition rate. At first, I designed a single-channel readout prototype that later was expanded into a multi-channel board. Figure 3 shows a picture of this four-channel assembly in which the diamond sensor is placed in the center. For this configuration we used a 4.0 x 4.0 mm<sup>2</sup> and 43  $\mu\text{m}$  thick diamond sensor.

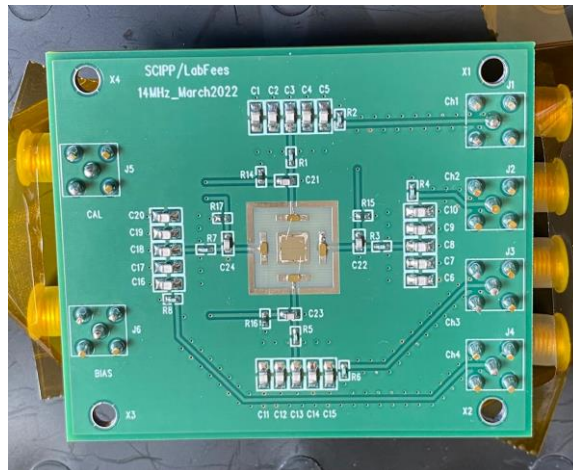


Figure 3: Picture of the four-channel quadrant diamond assembly used to measure the position resolution of the XPP X-ray beam at SLAC.

I participated directly in testing this four-channel readout system at the XPP X-ray beam at SLAC. Figure 2 shows the sweep trajectory of the X-ray beam across two quadrants of the sensor as we read the signals generated at each interval. During the beam test, X-ray pulses in the range of 1 nJ - 15 nJ were recorded, giving me access to information about the charge collected across quadrant 3 and 4. Once I acquired the charge collection deposited by the beam for 4 nJ average X-ray pulses, I was able to calculate the charge resolution of the readout system to be about 0.025 pC. Following that, I obtained the values corresponding to the asymmetry and computed the position resolution of this device in the order of 3.5  $\mu\text{m}$ . Considering the FWHM of the X-ray beam to be about 350  $\mu\text{m}$ , the position resolution is about 1 % for pulse intensities of 4 nJ. Figure 4 below displays the measured XPP beam jitter in one-dimension for pulse-by-pulse at 50 MHz repetition rate.

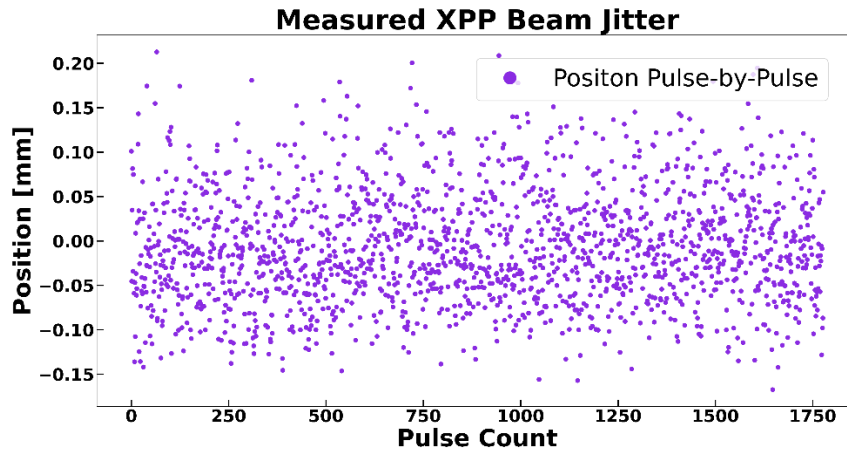


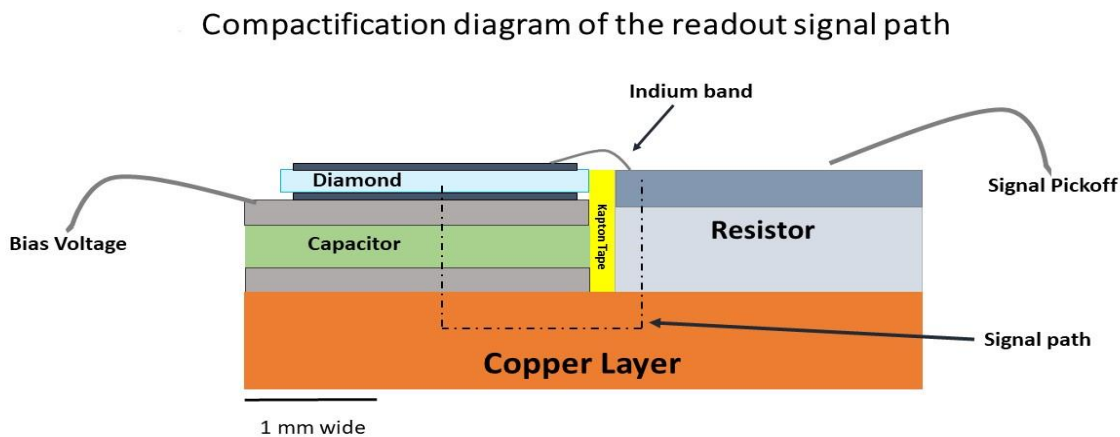
Figure 4: Measurement of the jitter of the LCLS XPP beam performed with the 50 MHz diagnostic system.

### Multi-GHz Readout of Solid-State Sensors

Lastly, I have been working in developing a solid-state sensor readout system capable of measuring XFEL pulses with repetition rates of 10 GHz. In a previous study published in the Journal of Synchrotron Radiation [1], we presented the characterization of a diamond sensor in terms of plasma density. In that paper, we found that at plasma densities above  $10^{16}$  charges/cm<sup>3</sup> the efficiency of the diamond detector degrades and the charge collection time increases. These space-charge effects can also be viewed as short-term radiation damage product of the high flux X-ray beam passing through a punctual volume across the sensor. Nevertheless, the study presented in that paper makes use of a readout system capable of reading XFEL pulses in the 1 GHz repetition rate. Although the study was below our goal to reach 10 GHz repetition rate, this gave us the opportunity to expand our knowledge in the electronic limits to transport fast signals.

Since reaching the multi-GHz electronic performance has a more difficult application, we have divided the task into four areas. 1) Understand the charge collection properties of diamond sensors. 2) How fast the signal can return to ground without being affected by self-resonances. 3) What kind of signal processing techniques can be applied for high-speed electronics. 4) Developing the interface between signal path and signal processing without signal degradation. As part of the Advanced Accelerator Diagnostics (AAD) group, I took a primary role together with my advisor Bruce Schumm and the electronic specialist, Max Wilder, on tackling the second

challenge point. Therefore, we began the design of an ultra-fast compact signal path prototype capable of transporting multi-GHz signals. Figure 5 shows a diagram of the mm-scale compact signal path designed at Santa Cruz Institute for Particle Physics (SCIPP). The goal is to make a signal path as small as possible by making use of special components such as single-layer capacitors and back-contact resistors. As shown in the figure 5, the signal will begin inside the diamond sensor, transfer across a low impedance indium band to the top part of the back-contact resistor, move down straight to ground, coming back across the single-layer capacitors, and returning to the back part of the diamond sensor. By completing the signal path in a small loop, we anticipate minimizing as much as possible the inductance contribution of the whole system.



1

Figure 5: Diagram of the ultra-fast signal path compact system developed at SCIPP, UC Santa Cruz. Special components such as single layer capacitor and back-contact resistors are represented in this diagram.

Although this ultra-fast compact signal path was designed using basic physics and electronic principles, we were not sure if the performance of this compact prototype would be optimal for our high-bandwidth goal. For that reason, we decided to implement a 3D RF simulator to help us understand the limitations and advantages this ultra-fast assembly has. Currently, I am using the 3D RF simulation software High Frequency Structure Simulation (HFSS) program provided by Ansys, Inc. This program uses discrete solutions to Maxwell's equations and provides us with the essential high-frequency electronic models to generate current/voltage transient signals. With the implementation of HFSS, we anticipate developing better understanding of different electronic features that could potentially affect our performance in the multi-GHz regime. Figure 6 shows a simple model created on HFSS containing the main components of the compact signal system. Here, we can observe that all the elements are placed as close as possible since the goal is to minimize the signal path and reduce any inductance contributions. This model is built using one  $2 \times 2 \text{ mm}^2$  diamond-based sensor ( $35 \text{ }\mu\text{m}$  thickness) containing platinum electrodes on the top and bottom. Six single-layer capacitors sit under the diamond sensor and make direct contact with the metal ground layer. The  $10 \text{ }\Omega$  back-contact resistor is connected from the sensor and to the ground using indium bands, which are characterized to have much lower impedance

contributions compared to normal bond wires. The assembly sits on top of a copper metal layer, which then sits on top of a high-frequency material called Rogers 4350. This material is used to reduce the self-resonances the system can generate when high-bandwidth signals propagate around.

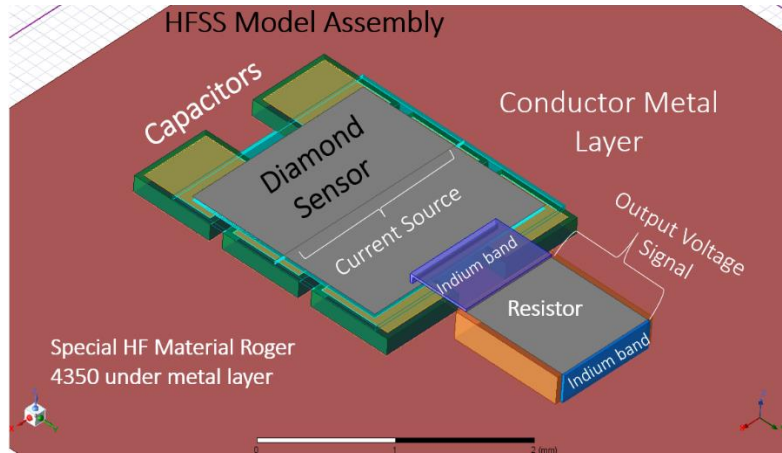


Figure 6: Diagram of the ultra-fast compact signal assembly created on HFSS.

Figure 7 shows the signal response across the back-contact resistor when the resistance varies from  $1 \Omega$  to  $15 \Omega$ . Although these results are preliminary, we can see how beneficial HFSS will be for us to make changes needed to optimize the assembly’s performance.

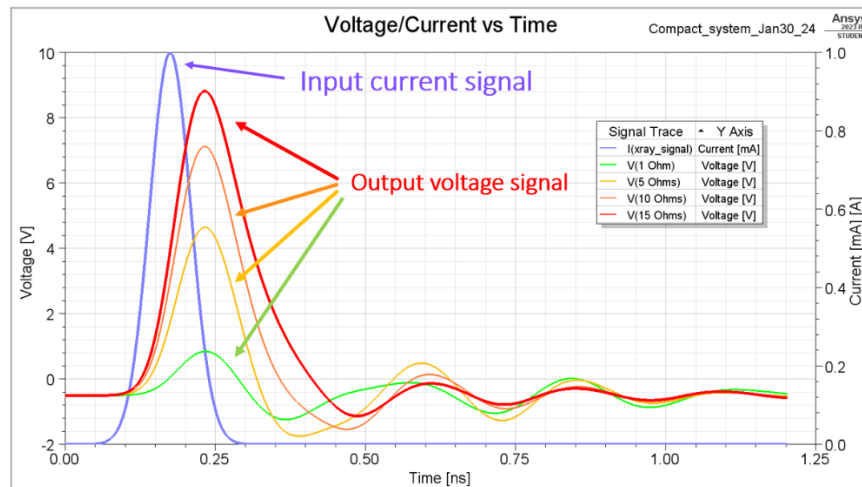


Figure 6: Input current transient signal and voltage output responses when varying the back-contact resistor values.

HFSS seems to be the right software to explore as we move forward in the development of new prototypes capable of performing at high-frequency and providing the adequate diagnostic response we are aiming for. I am planning to continue my capacitation with HFSS and use it to generate more simulations that can help the AAD collaboration group. I would like to thank the HEPCAT program for providing me with the resources to continue this incredible work and enabling me to pursue my Ph.D. in accelerator physics and R&D in instrumentation.

### References

- [1] J. Bohon, et al. "Use of diamond sensors for a high-flux, high-rate X-ray pass-through diagnostic." *J. Synchrotron Radiat.*, vol. 29, pp 595-601, 2022. doi: 10.1107/s1600577522003022